Journal of Nuclear Medicine, published on August 19, 2021 as doi:10.2967/jnumed.121.262395

^{18}F-fluorocholine PET/CT is more sensitive than ^{11}C-methionine PET/CT for the localization of hyperfunctioning parathyroid tissue in primary hyperparathyroidism

Céline Mathey [1], Caroline Keyzer [2], Didier Blocklet[1], Gaetan Van Simaeys [1], Nicola Trotta [1], Simon Lacroix[1], Bernard Corvilain[3], Serge Goldman [1], Rodrigo Moreno-Reyes [1]

Department of [1]Nuclear Medicine and PET/biomedical Cyclotron Unit, [2]Medical Imaging, [3]Endocrinology

Hôpital Érasme, Université libre de Bruxelles, Brussels, Belgium.

Address correspondence and reprint requests to:

Céline Mathey, department of Nuclear Medicine,

Hôpital Érasme, route de Lennik 808, B-1070, Brussels, Belgium.

Tel: +32-2-555-5727

Fax: +32-2-555-4701

e-mail: Celine.Mathey@erasme.ulb.ac.be.

Manuscript word count: 5561 words

Short running title:

FCH- vs. MET-PET in hyperparathyroidism

ABSTRACT

Purpose: Preoperative molecular imaging is paramount to direct surgery in primary hyperparathyroidism (pHTP). We investigate the diagnostic performance of ^{18}F-fluorocholine (^{18}F-FCH) PET/CT compared to ^{11}C-methionine (^{11}C-MET) PET/CT for the localization of hyperfunctioning parathyroid tissue in patients with pHTP and negative or inconclusive ^{99m}Tc-sestaMIBI SPECT (MIBI) findings.

Materials and Methods: Fifty-eight patients with biochemical evidence of pHTP and negative or inconclusive MIBI were referred for pre-surgical detection and localization of hyperfunctioning parathyroid tissue by ^{11}C-MET- and ^{18}F-FCH-PET/CT. The PET/CT results were classified into 3 categories (positive, inconclusive or negative) based on the nodular aspect of tracer uptake and the visualisation of corresponding nodules on CT. The PET/CT results were correlated with the surgical and histopathological findings used as gold standard.

Results: Fifty-three patients were included for analysis. ^{18}F-FCH-PET/CT was positive in 39 patients (74%), inconclusive in 5 (9%) and negative in 9 (17%), compared to 25 (47%), 12 (23%) and 16 (30%) respectively for ^{11}C-MET-PET/CT. ^{18}F-FCH localized 11 additional foci (6 positive and 5 inconclusive) compared to ^{11}C-MET.

Twenty-six patients (sex F/M ratio16/10) underwent surgery with resection of 31 lesions (22 adenomas, 6 hyperplastic glands, 3 carcinomas) and 1 normal gland. At follow-up, twenty-one (81%) patients were considered cured after surgery, while 3 (12%) patients had persistence of hypercalcaemia. With inconclusive cases being considered as negative, ^{18}F-FCH-PET/CT correctly localized 26 lesions in 24/26 (92%) patients compared to 16 lesions in 15/26 (58%) patients localized by ^{11}C-MET-PET/CT. Per patient-based sensitivity and positive predictive value (PPV) were 96% and 96% for ^{18}F-FCH and 60% and 94% for ^{11}C-MET ($p<0.0001$). Per lesion-based sensitivity and PPV were respectively 84% and 90% for ^{18}F-FCH vs. 52% and 94% for ^{11}C-MET ($p<0.0001$).

Conclusion: In the presence of biochemical evidence of pHTP with negative or inconclusive MIBI, ^{18}F-FCH-PET/CT has a better performance than ^{11}C-MET-PET/CT for the detection of pathological parathyroid tissue, allowing localization of parathyroid adenoma or hyperplasia in 96% of patients.

Key words Primary hyperparathyroidism; Parathyroid adenoma; ^{18}F-fluorocholine; ^{11}C -methionine; PET/CT.

INTRODUCTION

Primary hyperparathyroidism (pHPT) is one of the most frequent endocrine disorders with a prevalence of about 2% in women older than 50 y. Long-term consequences of pHPT affect mainly the skeleton (osteoporosis, fractures), and the kidney (nephrolithiasis, impaired renal function). Diagnosis is based on increased serum calcium, low phosphorus levels, and inappropriate parathyroid hormone (PTH) levels *(1*). Primary hyperparathyroidism is associated with a solitary parathyroid adenoma in 80-90% of patients or more rarely multiglandular disease (MGD) or diffuse parathyroid hyperplasia *(1)*.

Optimal management of pHPT consists in the pre-operative localization of the abnormal parathyroid gland allowing for minimally invasive parathyroidectomy *(2,3)*. Conventional first-line pre-surgical imaging is based on ^{99m}Technetium-sestaMIBI parathyroid scintigraphy (MIBI) with subtraction images, usually complemented by ultrasonography. It ideally includes single-photon emission computed tomography/X-ray computed tomography (SPECT/CT) acquisition, with a detection rate of 84-88% *(4,5)*.

Currently, in case of negative/equivocal scintigraphy results, discrepant results with the ultrasonography or persistence/recurrence of HPT after surgery, an alternative investigation is recommended, involving hybrid positron emission tomography/X-ray computed tomography technique (PET/CT), usually with amino-acid tracers, such as ^{11}C-methionine (^{11}C-MET) *(6,7)*. Use of PET/CT for that purpose offers a shorter acquisition time, and higher spatial resolution and sensitivity *(8)*. Meta-analyses reported sensitivity of ^{11}C-MET between 77-81% in a per patient-based analysis in patients with pHPT and negative/inconclusive MIBI SPECT *(6,9)*. However, short half-life of ^{11}C-MET imposes on-site production and strict acquisition conditions *(6)*.

More recently,^{18}F-fluorocholine (^{18}F-FCH) PET/CT used for imaging prostatic neoplasia assessment *(10)* has been shown capable to localize abnormal parathyroid gland in patients with negative/inconclusive MIBI SPECT studies *(3,8,11,12)*. It has the advantages over ^{11}C-MET of a longer half-time and a more favorable positron energy. Choline is a precursor of phospholipids that are essential constituents of cellular lipidic structures. ^{18}F-FCH is therefore a tracer of lipid metabolism whose uptake increases following increased intracellular metabolism requiring synthesis of phospholipids.

The aim of this study was to investigate if, in patients with primary hyperparathyroidism and negative/inconclusive MIBI, the diagnostic performance of ^{18}F-FCH-PET/CT is not inferior to the one of ^{11}C-MET-PET/CT in a preoperative perspective. The secondary objective of the study was to compare the two methods for their performance in the detection of individual hyperfunctioning parathyroid lesions.

MATERIALS AND METHODS

Patients

Between November 2015 and December 2018, we included prospectively 58 patients with biologically proven pHPT (hypercalcemia and elevated or inappropriately normal PTH levels) and negative or inconclusive MIBI imaging performed in various institutions, including ours, and involving SPECT with or without combined CT.

Upon inclusion and in case of absence of a recent blood test (< 3 months) confirming hyperparathyroidism, a blood sample was taken in order to measure serum values of calcium, phosphorus, PTH, albumin and vitamin D. Serum calcium level was measured the days following surgery in order to check for normalization.

Institutional ethics committee approval was obtained before the start of this prospective study and all subjects signed an informed consent form (P2015/307).

PET/CT Procedure

All PET/CT were performed on a Gemini GXL (n=15) or a TF64 Philips (n=38) PET/CT camera (Philips Medical Systems, Cleveland, Ohio, USA), with essentially identical protocols on both systems. All patients underwent sequentially a ^{11}C-MET- and a ^{18}F-FCH-PET/CT (Supplemental Fig 1).

^{11}C-*MET-PET/CT*. All patients were injected with an average bolus of 555 MBq of ^{11}C-MET in a fasted state. Fifteen minutes after injection, an unenhanced CT (40 mAs, 120 kV, slice thickness 2.0 mm, interval 1.5mm) was performed, followed by PET acquisition of the neck and upper mediastinum (3 bed positions, 7 min per bed position). Images were reconstructed with 2 different algorithms depending on the PET camera (LOR-RAMLA or BLOB-OS-TF).

^{18}F-*FCH-PET/CT*. Approximately 3 hours after ^{11}C-MET injection, an unenhanced CT (40mAs, 120kV, slice thickness 2.0 mm, interval 1.5mm) was acquired. Then, with the patient lying in the PET/CT tomograph, 4 MBq/kg of body mass of ^{18}F-FCH was administered intravenously. ^{18}F-FCH was prepared in 2 steps using a fully automated radiochemistry synthesizer (Trasis All-in-One, Ans, Belgium)*(13)*. A 15-min dynamic PET acquisition covering the neck was started at time of tracer injection, followed by a static acquisition (early ^{18}F-FCH - ^{18}F-FCH$_E$) on the neck and the upper mediastinum (3 bed positions, 7 min per bed position). PET/CT imaging of the neck and upper mediastinum was repeated 60 min after injection (late ^{18}F-

FCH – ^{18}F-FCH$_L$) and used for image analysis in the present work. Images were reconstructed with 2 different algorithms depending on the PET camera (LOR-RAMLA or BLOB-OS-TF).

Images Interpretation. All PET/CT images were analyzed independently by a nuclear medicine physician (11 years of experience) and a radiologist (18 years of experience), who were aware of previous imaging and laboratory findings of the patients and a nuclear medicine physician (27 years of experience) blinded to any clinical and imaging information. Discordant image interpretation occurred in 11 patients. In all of these cases, a consensus reading led to a final common interpretation. There was no pause between ^{18}F-FCH and ^{11}C-MET readings.

The images (MIP and 3D volume) were evaluated visually to determine the number and exact location of uptake areas suggestive of hyperfunctioning parathyroid glands. The results were classified into 3 categories based on the aspect of the tracer uptake area and the visualization of corresponding nodules on the CT: (a) positive, in case of a clear circumscribed uptake area on PET images or a faint circumscribed uptake area corresponding to a nodular lesion on CT; (b) inconclusive, in case of a faint uptake area with no corresponding nodule on CT; (c) negative, in case of no discernable tracer uptake area. Lesion localization was assigned to six anatomical regions: right and left upper (P4), right and left lower (P3), intrathyroidal and ectopic. In case of a discrepancy between readers' assessments, the appropriate category and anatomical localization were assigned by consensus.

The semi-quantitative analysis was performed with Philips IntelliSpace Portal software (ISP, version 9). The maximum and mean standardized uptake values of the parathyroid lesion (PA) were measured (SUVmax PA and SUVmean PA). We estimated the contrast between the lesion and the thyroid using the SUVmax PA/SUVmean Thyroid ratio (PA/Thyroid). By this ratio, we evaluated the capacity to identify the parathyroid activity close to the organ it usually lies behind. SUVmax Thyroid and SUVmean Thyroid were measured by placing a spherical VOI of 1cm³ in diameter on the contralateral thyroid lobe unless morphologically pathological or right lobe in the absence of lesion.

Surgery and Histology

Surgeons were aware of ^{11}C-MET- and ^{18}F-FCH-PET/CT data for all patients. They used this information to direct the surgical procedure, which was an open minimal invasive parathyroidectomy in case of a single area of uptake in ^{11}C-MET- or ^{18}F-FCH-PET/CT. If multiple lesions or an ectopic location were suspected, the surgical approach was adapted. In case of coexisting multinodular goiter or suspicious thyroid nodule(s), an additional hemi-thyroidectomy or total thyroidectomy was

performed. All operated cases had at least one lesion categorized as positive on either the ^{11}C-MET- or the ^{18}F-FCH-PET/CT, except for one patient with negative PET/CT in which full surgical exploration was decided for recurrent pHPT.

The results of ^{11}C-MET- and ^{18}F-FCH-PET/CT were compared to the surgical exploration and histopathological findings. Surgical success was established according to normalization of postoperative serum calcium level.

Statistical Analysis

Quantitative variables are expressed as mean +/- SD for normally distributed continuous variables and as median with 25th and 75th percentiles for non-normal continuous variables.

For the sake of comparison, negative, inconclusive and positive lesions were scored 0, 1 and 2, respectively. Tracer comparison of visual scoring performance was evaluated with Wilcoxon matched-pairs signed rank test. For visual decision performance on matched pairs of ^{11}C-MET- and ^{18}F-FCH-PET/CT images, inconclusive results were considered as negative, and McNemar's test with the continuity correction was used.

The sensitivity and positive predictive value (PPV) of PET/CT imaging were evaluated on a per-lesion and per-patient basis and calculated using histology analysis as the gold standard. Since no histological data were available in most patients with negative results on PET/CT, specificity and negative predictive values were not evaluated.

The D'Agostino & Pearson and Shapiro-Wilk tests were used to assess the normality of the sample values. Repeated measures of each relevant quantitative parameter (SUVmax PA, PA/Thyroid) were analyzed with the Friedman test. Dunn's tests were subsequently applied for multiple comparisons between tracers (^{11}C-MET, ^{18}F-FCH$_E$, ^{18}F-FCH$_L$). Nonparametric Spearman correlation r was calculated between early and late ^{18}F-FCH PET/CT with respect to ^{11}C-MET images for PA/Thyroid. After exclusion of negative cases, simple linear regression was further calculated to evaluate how this quantitative parameter vary in early and late ^{18}F-FCH PET/CT with respect to the corresponding parameter on ^{11}C-MET images. Runs tests were performed to assess lack of fit. Goodness of fit was assessed with R2. Statistical analyses were performed using GraphPad Prism 9.0 (GraphPad Software, La Jolla, California, USA) and its online McNemar's test calculator. For all tests, a P-value of less than 0.05 was considered statistically significant.

RESULTS

Among 58 patients that prospectively underwent a ^{11}C-MET- and ^{18}F-FCH-PET/CT, 53 patients were included in the analysis (Fig 1). Five patients were excluded because of unconfirmed pHPT (n=4) or technical problems (n=1). The

characteristics of the 53 patients are summarized in Table 1. Among them, 7 had a previous history of parathyroidectomy and persistent or recurrent pHPT. Four cases of familial pHPT were included, 3 of whom with previous surgery. Participants underwent ^{11}C-MET- and ^{18}F-FCH-PET/CT on the same day, except for 7 patients who had their two PET/CT imaging within 5 months. Twenty-six patients (16 females and 10 males) had parathyroidectomy with a histopathological confirmation of the presence of adenoma or hyperplasia in 24 patients. Fourteen patients had negative (9/53) or inconclusive (5/53) PET/CT results. Goiter was present in 10 patients (19%) and 29 patients had nodular thyroid disease (55%).

^{18}F-FCH-PET/CT Outperforms ^{11}C-MET-PET/CT for Lesion Localization at Both Early and Late Time Points in the Prospect of Surgery Guidance

^{18}F-FCH-PET/CT was positive in 39 patients (74%) and inconclusive in 5 patients (9%) compared to 25 patients (47%) and 12 patients (23%) respectively for ^{11}C-MET-PET/CT (Table 2). Visual scoring performance of ^{18}F-FCH-PET/CT was very superior over ^{11}C-MET-PET/CT on per-patient basis (Wilcoxon $P < 0.0001$). Also, McNemar's test of matched pairs discordant results also demonstrated the superiority of ^{18}F-FCH- over ^{11}C-MET-PET/CT in visual decision performance on per-patient basis (P value = 0.0005; chi-squared = 12.071 with 1 degree of freedom), with 14 patients positive only with ^{18}F-FCH-PET/CT, no patient positive only with ^{11}C-MET-PET/CT, whereas 25 patients were positive and 14 were negative with both tracers. Out of 26 patients with negative or inconclusive MIBI and positive PET/CT (either ^{11}C-MET- or ^{18}F-FCH-) who had surgery, 17 were switched from a cervical exploration to a MIP approach.

In 24 of 26 (92%) patients who had surgery, hyperfunctioning parathyroid tissue (adenoma/ hyperplasia/cancer) was correctly localized with ^{18}F-FCH (26 lesions), compared to 15 patients with ^{11}C-MET (16 lesions). On a per-patient basis, the PPV was 96% for ^{18}F-FCH and 94% for ^{11}C-MET. One patient was negative on both PET/CT and underwent a surgical exploration allowing the resection of a PA followed by calcemia normalization. No hyperfunctioning parathyroid tissue was found in a patient with persistent pHPT after surgery. Per-patient sensitivity of ^{18}F-FCH-PET/CT was 96% compared to 60% for ^{11}C-MET-PET/CT ($p<0.0001$). In addition, 5 patients had multiglandular disease detected on ^{18}F-FCH-PET/CT (19%). Postoperative calcemia used to define therapeutical success was obtained at 11.5 +/- 6.9 months post-surgery. A total of 21 (81%) patients who underwent parathyroidectomy were considered cured, 3 (12%) patients had recurrent or persistent hypercalcemia and 2 patients were lost to follow-up.

The comparison of lesion visual scoring performance between the two tracers is reported in Supplemental Table 1. ^{18}F-FCH-PET/CT detected a single uptake area in 37/53 patients and multiple uptake areas in 7/53 patients. On per-lesion basis

(Table 2), ^{18}F-FCH-PET/CT showed 47 positive and 9 inconclusive uptake areas. ^{18}F-FCH-PET/CT allowed detection of 11 additional uptake areas (6 positive and 5 inconclusive) compared to ^{11}C-MET-PET/CT. Thirteen inconclusive uptake areas on ^{11}C-MET were positive on ^{18}F-FCH. Three ectopic parathyroid glands in the superior mediastinum and 2 intrathyroidal localizations were identified with both PET tracers. Comparison of tracers for visual scoring performance on a per-lesion basis revealed the superiority of ^{18}F-FCH- over ^{11}C-MET-PET/CT (Wilcoxon $P < 0.0001$). Again, McNemar's test revealed as well the superiority of ^{18}F-FCH- over ^{11}C-MET-PET/CT for visual decision performance on a per-lesion basis (P value < 0.0001; chi-squared = 17.053 with 1 degree of freedom), with 19 lesions positive only with ^{18}F-FCH-PET/CT, no lesion positive only with ^{11}C-MET-PET/CT, whereas 28 lesions were positive and 18 were negative with both tracers. Except for two lesions with rapid washout only visualized on ^{18}F-FCH$_E$, and one uncertain lesion only found on ^{18}F-FCH$_L$, all lesions were visualized on early and late acquisitions, without significant difference in visual scoring assessment of contrast. Two cases are illustrated in Supplemental Fig 2.

A total of 31 glands were surgically removed and histology revealed 22 parathyroid adenomas, 6 hyperplastic glands and 3 parathyroid carcinomas (Supplemental Table 2). Locations of removed glands are listed in Supplemental Table 1.

All localizations described on the PET/CT were concordant with surgery, except for one patient with a multiple endocrine neoplasia (MEN1) in which the uptake area was found in the lower left retropolar region on PET/CT, while the parathyroid adenoma was identified in the lower right retropolar region; two normal glands were also surgically removed on the left in this patient. In another patient with multiple foci observed on ^{18}F-FCH and ^{11}C-MET, pathological tissue had been probably left in place because he was not cured after removal of one correctly localized lesion (HP) and two thyroid nodules. One uptake area found on both PET/CT was not explored during surgery, and in 4 cases, parathyroid hyperplasia was found in false negative ^{18}F-FCH-PET/CT locations. On a per-lesion basis (Supplemental Table 2), sensitivity and PPV were 84% and 90% for ^{18}F-FCH-PET/CT, respectively, and 52% and 94% for ^{11}C-MET-PET/CT ($p<0.0001$).

Contrast-to-Thyroid and PA Uptake Are Significantly Higher with ^{18}F-FCH-PET/CT Compared to ^{11}C-MET-PET/CT

The visual comparison of the contrast-to-background in the detected anomalies for ^{18}F-FCH and ^{11}C-MET revealed a superiority of ^{18}F-FCH over ^{11}C-MET, both at early and late imaging times (Supplemental Fig 3). Higher uptake was observed in 71-82% (39-45/55) of anomalies in ^{18}F-FCH compared to ^{11}C-MET and a similar uptake of the 2 tracers was observed in 25% (14/55) and 16% (9/55) of cases for ^{18}F-FCH$_E$ and ^{18}F-FCH$_L$ respectively. When we only consider the cases

that underwent parathyroidectomy, we found similar proportions. Only 1 case operated on had a lesion better visualized on ^{11}C-MET- than on ^{18}F-FCH-PET/CT.

Supplemental Fig 4 shows the distribution of SUVmax PA and PA/Thyroid for each tracer. SUVmax PA on ^{18}F-FCH$_E$ and ^{18}F-FCH$_L$, given as median (P25-P75), was 3.26 (2.45-4.74) and 3.52 (2.58-4.91), respectively, while the median SUVmax PA on ^{11}C-MET was 1.51 (0.96-2.73). So, the SUVmax PA on ^{18}F-FCH$_E$ and ^{18}F-FCH$_L$ were approximatively twice higher than ^{11}C-MET SUVmax ($p<0.0001$). There was no statistically significant difference between SUVmax PA and PA/Thyroid on ^{18}F-FCH$_E$ and ^{18}F-FCH$_L$ ($p=0.3569$). PA/Thyroid on ^{18}F-FCH$_E$ and ^{18}F-FCH$_L$ were 1.39 (1.29-1.54) and 1.39 (1.29-1.68), respectively ($p = 0.1005$). The quantitative analysis resulted in non-significant differences for both SUVmax and PA/Thyroid between adenoma and hyperplasia on both ^{18}F-FCH- and ^{11}C-MET-PET/CT.

We observed a positive correlation between PA/Thyroid on ^{11}C-MET- and ^{18}F-FCH-PET/CT, despite the difference in the incorporation mechanisms (Fig 2). Linear fit revealed that PA/Thyroid was 11% higher in ^{18}F-FCH$_E$ and 31% higher in ^{18}F-FCH$_L$ compared to ^{11}C-MET: for ^{18}F-FCH$_E$, $r = 0.6843$, slope of 1,11 and intercept of 0,0175, $r^2 = 0,79$; for ^{18}F-FCH$_L$, $r = 0.5665$, slope of 1,315 and intercept of 0,046, $r^2 = 0,75$.

DISCUSSION

To the best of our knowledge, this is the first study comparing ^{11}C-MET and ^{18}F-FCH tracers for the preoperative detection and localization of hyperfunctioning parathyroid tissue. Our results demonstrate the diagnostic superiority of ^{18}F-FCH- over ^{11}C-MET-PET/CT for parathyroid adenoma/hyperplasia detection in patients with negative or inconclusive MIBI exploration.

Precise preoperative localization of hyperfunctioning parathyroid gland is a prerequisite for efficient minimally invasive surgery. For this purpose, PET/CT recently emerged as a complementary second-line imaging technique with the advantage of a higher resolution associated with PET compared to SPECT, as well as a shorter acquisition time *(14)*.

Several publications concluded on a better diagnostic performance of ^{18}F-FCH- and ^{11}C-MET-PET/CT for the localization of parathyroid lesions, in comparison to conventional imaging methods *(3,7,8,11,15–17)*. The present study confirms the added value of this new tracer in the detection and precise localization of hyperfunctioning parathyroid tissue in the subgroup of patients with pHPT and negative/ inconclusive MIBI with SPECT. The sensitivity of ^{18}F-FCH-PET/CT was 96% on a per-patient basis and 84% on a per-lesion basis. As in the APACH study, we considered the histopathological results as the gold-standard for per-lesion analyses *(8)*. Our findings are comparable with those reported in previous studies. A recent meta-analysis *(18)* concluded on pooled sensitivity of 93.7% and 91.3% on patient-based and lesion-based analyses, respectively. The detection rate of lesions were between 77-94% (on patient-basis) and 80-96% (on lesion-basis) *(15)*.

Our cohort includes patients for whom the choice of surgical management was challenging (familial hyperparathyroidism, relapsing or persistent HPT, multiglandular forms) compared to most previous studies. Five of the 6 patients with persistent/relapsed postsurgical pHPT had abnormal uptake areas revealed by ^{18}F-FCH and we detected 19% of histologically confirmed multiglandular diseases. Still, the majority of our patients presented with a confirmed solitary lesion (81%), which was consistent with the rate reported in the literature (74% in Beheshti et al.*(5)*). There was no SUVmax cut-off value in ^{18}F-FCH that could be set to distinguish PA from HP.

The optimal time point for ^{18}F-FCH image acquisition remains controversial *(3,17,19,20)*. This results from a 3-phase temporal pattern of ^{18}F-FCH PA uptake, with an early washout, followed by an intermediate phase of stability and a late phase of increase *(21)*. We therefore opted for a dual time-point mode of acquisition in this study. Based on the visual evaluation of the images and the analysis of PA/Thyr, i.e. a target-to-background ratio, we did not better discern lesions on the late images compared to the early ones. Rep et al. *(17)* described in late acquisition images a greater accumulation of ^{18}F-FCH in PA compared to the thyroid, with a slightly slower decrease in signal, translating in a better lesion contrast. In agreement with our

results, Broos et al. *(19)* reported a decrease in absolute uptake in PA over time with an increase in contrast relative to the thyroid because of a weaker retention in the latter. Conversely, Michaud et al.*(16)* concluded that late images did not yield additional findings over early ones. Noticeably, in all previous studies, early images were acquired at 5 min post-injection, while we decided for a slightly later acquisition. We found two patients with lesions showing a rapid ^{18}F-FCH washout in our population. Nevertheless, since most parathyroid lesions were observed on both acquisitions, we recommend performing acquisition at 15 min, reserving an additional late imaging for patients whose early acquisition is negative or inconclusive, as also suggested by Uslu-Besli *(22)*.

Before ^{18}F-FCH, ^{11}C-MET has been widely used as a reliable second-line agent in pHPT. Overall, in our study, ^{18}F-FCH showed a significantly higher sensitivity, with more cases diagnosed and with increased accuracy, compared to ^{11}C-MET. The advantage of ^{18}F-FCH imaging over ^{11}C-MET imaging seems to be strongly related to the fact that it produces more conclusive data. Indeed, 13 anomalies judged as "inconclusive" on ^{11}C-MET-PET/CT were considered as positive on the ^{18}F-FCH-PET/CT. The superior imaging qualities of ^{18}F-labeled radiotracers over ^{11}C-labeled ones probably participate to this better performance of ^{18}F-FCH. Apart from an effect of the positron energy, differences in molecular properties and uptake mechanisms involved probably explain the differences in diagnostic performance between ^{18}F-FCH and ^{11}C-MET. Indeed, the two tracers explore very different biochemical pathways. ^{11}C-MET uptake most probably depends on expression and activity of amino-acid transporters such as LAT1, and secondarily on its incorporation in the protein pre-pro-PTH. So, ^{11}C-MET uptake may be closely dependent on the level of synthesis and release of PTH. On the contrary, ^{18}F-FCH uptake enters chief cells – those responsible for PTH production – and oxyphilic cells of parathyroid tissue through a specific membrane transporter. After reaching the cytoplasm, ^{18}F-FCH is accumulated in the mitochondria in relation to its positive charge, as it is the case for MIBI. In the chief cells, ^{18}F-FCH is also phosphorylated by a a choline-kinase, which is overexpressed in patients with pHPT, leading to a phosphorylated form– i.e. phosphatidylcholine – incorporated into the cytoplasmic membrane. The fact that two different mechanisms favor ^{18}F-FCH incorporation into the PTH producing cells may represent an advantage over the other tracers such as ^{11}C-MET and MIBI *(23)*.

For the evaluation of patients with pHPT and negative/ inconclusive MIBI SPECT, a pooled sensitivity of 86% had been reported in a per patient-based analysis of ^{11}C-MET-PET/CT *(24)*. Two other meta-analyses reported sensitivity ranging from 69% to 81% and a detection rate per patient of 70% *(6,9)*. In our population, we reached a slightly lower sensitivity (60%), probably related to a high prevalence of clinical statuses that negatively influence the outcome of pre-surgical localization imaging, i.e. post-surgical recurrence and familiar forms of pHPT *(12,15)*. The visual analysis more frequently resulted in

inconclusive uptake on ^{11}C-MET- than on ^{18}F-FCH-PET/CT. Noticeably, as in other analyses *(11)*, we assimilated inconclusive results to negative ones because we considered that such results would preclude valuable image-guided planning of a minimally invasive parathyroidectomy. Such a position is not adopted by all authors *(8)*. Our study has some limitations. First, it did not directly compare ^{18}F-FCH-PET/CT to MIBI-SPECT/CT. Such analyses have already been made, showing the far superiority of ^{18}F-FCH imaging *(3,8,11,15–17)*. This comparison was not in the objectives of our study since we only selected patients with primary hyperparathyroidism and negative/inconclusive MIBI exploration. Consequently, our results cannot be extrapolated to patients with tertiary hyperparathyroidism, and it cannot determine to what extent ^{18}F-FCH should replace MIBI as first-line molecular imaging in pHPT. Also, not all patients underwent surgery after presurgical PET/CT. So, our findings on the diagnostic impact of ^{18}F-FCH-PET/CT only relate to the 26/53 patients in which histopathological data were available.

Finally, although ^{18}F-FCH-PET/CT shows good performances for hyperfunctioning parathyroid tissue localization, potential drawbacks must be considered before adopting this modality as the single pre-surgical imaging procedure in pHPT. As in previous studies *(12)*, we observed false-positive and false-negative findings. The 3 false-positive results related to one case of localization discordance between PET/CT and surgery, one case of uptake in a normal parathyroid gland and one case of uptake in a thyroid nodule. Even if all 3 cases are classified as false-positive due to the lack of histological evidence of PA or HP, 2 patients were not cured after surgery, leaving open the possibility that resection did not involve the lesions pointed out by ^{18}F-FCH-PET/CT. Five false-negative results concerned 4 cases of parathyroid hyperplasia and one patient with recurrent pHPT who ultimately had a PA resection during an extensive bilateral neck exploration. As in previous studies *(11,14,16)*, discordant PET/CT interpretation between readers occurred in 2 situations in which a nodular uptake was found within the thyroid gland. The differential diagnosis between a hypermetabolic thyroid nodule and an intrathyroidal parathyroid lesion appeared difficult due to the lack of comparison with a specific thyroid tracer *(14)*. Still, as illustrated in Fig 3 and Supplemental Fig 2, mild to moderate physiological ^{18}F-FCH uptake by the thyroid did not affect image interpretation in most of our cases, contrary to what has been reported *(5)*. Another source of potential misinterpretation (Supplemental Table 3) is the presence of reactive lymph nodes in classical locations of parathyroid adenomas. Globally, despite the high prevalence of nodular thyroid in our patients and the frequent occurrence of hypermetabolic lymph nodes, both ^{18}F-FCH- and ^{11}C-MET-PET/CT correctly localized the parathyroid lesions in the majority of surgically treated patients.

To determine which PET tracer should be privileged for a particular indication, various factors must be taken into account, including availability, diagnostic performance and duration of examination *(25)*. ^{18}F-FCH outperforms ^{11}C-MET for these three criteria.

CONCLUSION

Our study demonstrated that in the presence of biochemical evidence of pHTP with negative or inconclusive MIBI, ^{18}F-FCH-PET/CT has a better performance than ^{11}C-MET-PET/CT for the detection of pathological parathyroid tissue, allowing localization of parathyroid adenoma or hyperplasia in 96% of patients. Since ^{18}F-FCH has been proved to be superior to MIBI in previous studies, our results position ^{18}F-FCH-PET/CT as the modality of choice for lesion localization in pHPT.

DISCLOSURES

The authors declare they did not receive any funding for this study. No potential conflicts of interest relevant to this article exist.

KEY POINTS

Question Is ^{18}F-fluorocholine superior than ^{11}C-methionine PET/CT for the localization of hyperfunctioning parathyroid tissue in patients with primary hyperparathyroidism and negative or inconclusive ^{99m}Tc-sestaMIBI SPECT findings?

Pertinent Findings In this prospective clinical study, ^{18}F-fluorocholine correctly localized lesions in 92% of patients compared to 58% by ^{11}C-methionine.

Implications for Patient Care ^{18}F-Fluorocholine is more sensitive than ^{11}C-methionine for the localization of hyperfunctioning parathyroid tissue in patients with primary hyperparathyroidism and negative or inconclusive ^{99m}Tc-sestaMIBI SPECT.

REFERENCES

1. Hindié E, Zanotti-Fregonara P, Tabarin A, et al. The role of radionuclide imaging in the surgical management of primary hyperparathyroidism. *J Nucl Med.* 2015;56:737–44.

2. Bilezikian JP, Brandi ML, Eastell R, et al. Guidelines for the management of asymptomatic primary hyperparathyroidism: summary statement from the fourth international workshop. *J Clin Endocrinol Metab.* 2014;99:3561–9.

3. Lezaic L, Rep S, Sever MJ, Kocjan T, Hocevar M, Fettich J. ^{18}F-Fluorocholine PET/CT for localization of hyperfunctioning parathyroid tissue in primary hyperparathyroidism: a pilot study. *Eur J Nucl Med Mol Imaging.* 2014;41:2083–9.

4. Treglia G, Sadeghi R, Schalin-Jäntti C, et al. Detection rate of (99m) Tc-MIBI single photon emission computed tomography (SPECT)/CT in preoperative planning for patients with primary hyperparathyroidism: A meta-analysis. *Head Neck.* 2016;38 Suppl 1:E2159-2172.

5. Beheshti M, Hehenwarter L, Paymani Z, et al. 18F-Fluorocholine PET/CT in the assessment of primary hyperparathyroidism compared with 99mTc-MIBI or 99mTc-tetrofosmin SPECT/CT: a prospective dual-centre study in 100 patients. *Eur J Nucl Med Mol Imaging.* 2018;45:1762–71.

6. Kluijfhout WP, Pasternak JD, Drake FT, et al. Use of PET tracers for parathyroid localization: a systematic review and meta-analysis. *Langenbecks Arch Surg.* 2016;401:925–35.

7. Tang B-N-T, Moreno-Reyes R, Blocklet D, et al. Accurate pre-operative localization of pathological parathyroid glands using 11C-methionine PET/CT. *Contrast Media Mol Imaging.* 2008;3:157–63.

8. Quak E, Blanchard D, Houdu B, et al. F18-choline PET/CT guided surgery in primary hyperparathyroidism when ultrasound and MIBI SPECT/CT are negative or inconclusive: the APACH1 study. *Eur J Nucl Med Mol Imaging.* 2018;45:658–66.

9. Caldarella C, Treglia G, Isgrò MA, Giordano A. Diagnostic performance of positron emission tomography using ^{11}C-methionine in patients with suspected parathyroid adenoma: a meta-analysis. *Endocrine.* 2013;43:78–83.

10. Quak E, Lheureux S, Reznik Y, Bardet S, Aide N. F18-choline, a novel PET tracer for parathyroid adenoma? *J Clin Endocrinol Metab.* 2013;98:3111–2.

11. Michaud L, Burgess A, Huchet V, et al. Is 18F-fluorocholine-positron emission tomography/computerized tomography a new imaging tool for detecting hyperfunctioning parathyroid glands in primary or secondary hyperparathyroidism? *J Clin Endocrinol Metab.* 2014;99:4531–6.

12. Grimaldi S, Young J, Kamenicky P, et al. Challenging pre-surgical localization of hyperfunctioning parathyroid glands in primary hyperparathyroidism: the added value of 18F-Fluorocholine PET/CT. *Eur J Nucl Med Mol Imaging.* 2018;45:1772–80.

13. Otabashi M, Desfours C, Vergote T, Brichard L, Morelle J-L, Philippart G. Automated production of high purity [18F]Fluorocholine at high activity on the AllInOne Synthesizer. *J Nucl Med.* 2016;57(supplement 2):2732–2732.

14. Imperiale A, Taïeb D, Hindié E. 18F-Fluorocholine PET/CT as a second line nuclear imaging technique before surgery for primary hyperparathyroidism. *Eur J Nucl Med Mol Imaging.* 2018;45:654–7.

15. Kluijfhout WP, Vorselaars WMCM, van den Berk SAM, et al. Fluorine-18 fluorocholine PET-CT localizes hyperparathyroidism in patients with inconclusive conventional imaging: a multicenter study from the Netherlands. *Nucl Med Commun.* 2016;37:1246–52.

16. Michaud L, Balogova S, Burgess A, et al. A Pilot Comparison of 18F-fluorocholine PET/CT, ultrasonography and 123I/99mTc-sestaMIBI dual-phase dual-isotope scintigraphy in the preoperative localization of hyperfunctioning parathyroid glands in primary or secondary hyperparathyroidism: influence of thyroid anomalies. *Medicine.* 2015;94(41):e1701.

17. Rep S, Lezaic L, Kocjan T, et al. Optimal scan time for evaluation of parathyroid adenoma with [(18)F]-fluorocholine PET/CT. *Radiol Oncol.* 2015;49:327–33.

18. Evangelista L, Ravelli I, Magnani F, et al. 18F-choline PET/CT and PET/MRI in primary and recurrent hyperparathyroidism: a systematic review of the literature. *Ann Nucl Med.* 2020;34:601–19.

19. Broos W, Wondergem M, van der Zant F, Knol R. Dual-time-point 18F-fluorocholine PET/CT in parathyroid imaging. *J Nucl Med.* 2019;60:1605-10.

20. Jun G, Pampaloni MH, Villanueva-Meyer J, Ravanfar V, Suh I, Hope T. 18-F-fluorocholine PETMR: optimizing injection delay for parathyroid adenoma localization. *J Nucl Med.* 2018;59(supplement 1):236–236.

21. Morland D, Richard C, Godard F, Deguelte S, Delemer B. Temporal uptake patterns of 18F-fluorocholine among hyperfunctioning parathyroid glands. *Clin Nucl Med.* 2018;43:504–5.

22. Uslu-Beşli L, Sonmezoglu K, Teksoz S, et al. Performance of F-18 fluorocholine PET/CT for detection of hyperfunctioning parathyroid tissue in patients with elevated parathyroid hormone levels and negative or discrepant results in conventional imaging. *Korean J Radiol.* 2020;21:236–47.

23. Ferrari C, Santo G, Mammucci P, Pisani AR, Sardaro A, Rubini G. Diagnostic value of choline PET in the preoperative localization of hyperfunctioning parathyroid gland(s): a comprehensive overview. *Biomedicines*. 2021; 25:9:231.

24. Yuan L, Liu J, Kan Y, Yang J, Wang X. The diagnostic value of 11C-methionine PET in hyperparathyroidism with negative 99mTc-MIBI SPECT: a meta-analysis. *Acta Radiol.* 2017;58:558–64.

25. Giovanella L, Bacigalupo L, Treglia G, Piccardo A. Will 18F-fluorocholine PET/CT replace other methods of preoperative parathyroid imaging? *Endocrine.* 2021;71:285–97.

TABLES

TABLE 1
Patient characteristics

Characteristic	Value	Normal values
	N = 53	
Sex (M/F)	16/37	
Age (years)	58 ± 16	
BMI (kg/m²)	28.2 ± 5.5	
Prior parathyroidectomy	7 (13)	
Prior imaging		
MIBI SPECT-CT [N (%)]		
Negative	38 (72)	
Inconclusive	15 (28)	
US	35 (66)	
Other	9 (17)	
Baseline laboratory values		
PTH (ng/L)*	72.0 (54-101)	4-49
Calcium (mmol/L)*	2.67 (2.62-2.69)	2.12-2.62
Phosphor (mmol/L)	0.75 ± 0.17	0.81-1.45
25(OH)D_3 (ng/ml)	24.74 ± 8.97	30-80
^{11}C-MET results [N (%)]		
Positive	25 (47)	
Negative†	28 (53)	
^{18}F-FCH results [N (%)]		
Positive	39 (74)	
Negative†	14 (26)	
Surgical results (*N* = 26) [N (%)]		
Pathological parathyroid tissue found	24 (92)	
Biological normalization during follow-up	21 (81)‡	

BMI=Body mass index, MIBI=^{99m}Tc-sestaMIBI SPECT scintigraphy, US=ultrasonography, PTH=parathyroid hormone,25(OH)D3=25-hydroxycholecalciferol, ^{11}C-MET=^{11}C-Methionine, ^{18}F-FCH=^{18}F-Fluorocholine
* non-normal variables expressed as median (P25-P75) (to D'Agostino-Pearson omnibus test)
†Negative imaging includes negative or inconclusive results
‡2 patients were lost to follow-up

TABLE 2

Contingency tables

Per patient	**Positive ^{18}F-FCH**	**Negative ^{18}F-FCH**	**Total**
Positive ^{11}C-MET	25	0	25
Negative ^{11}C-MET	14	14	28
Total	39	14	53

Per lesion	**Positive ^{18}F-FCH**	**Negative ^{18}F-FCH**	**Total**
Positive ^{11}C-MET	28	0	38
Negative ^{11}C-MET	19	18	37
Total	47	18	75

^{18}F-FCH=^{18}F-Fluorocholine, ^{11}C-MET=^{11}C-Methionine

FIGURES

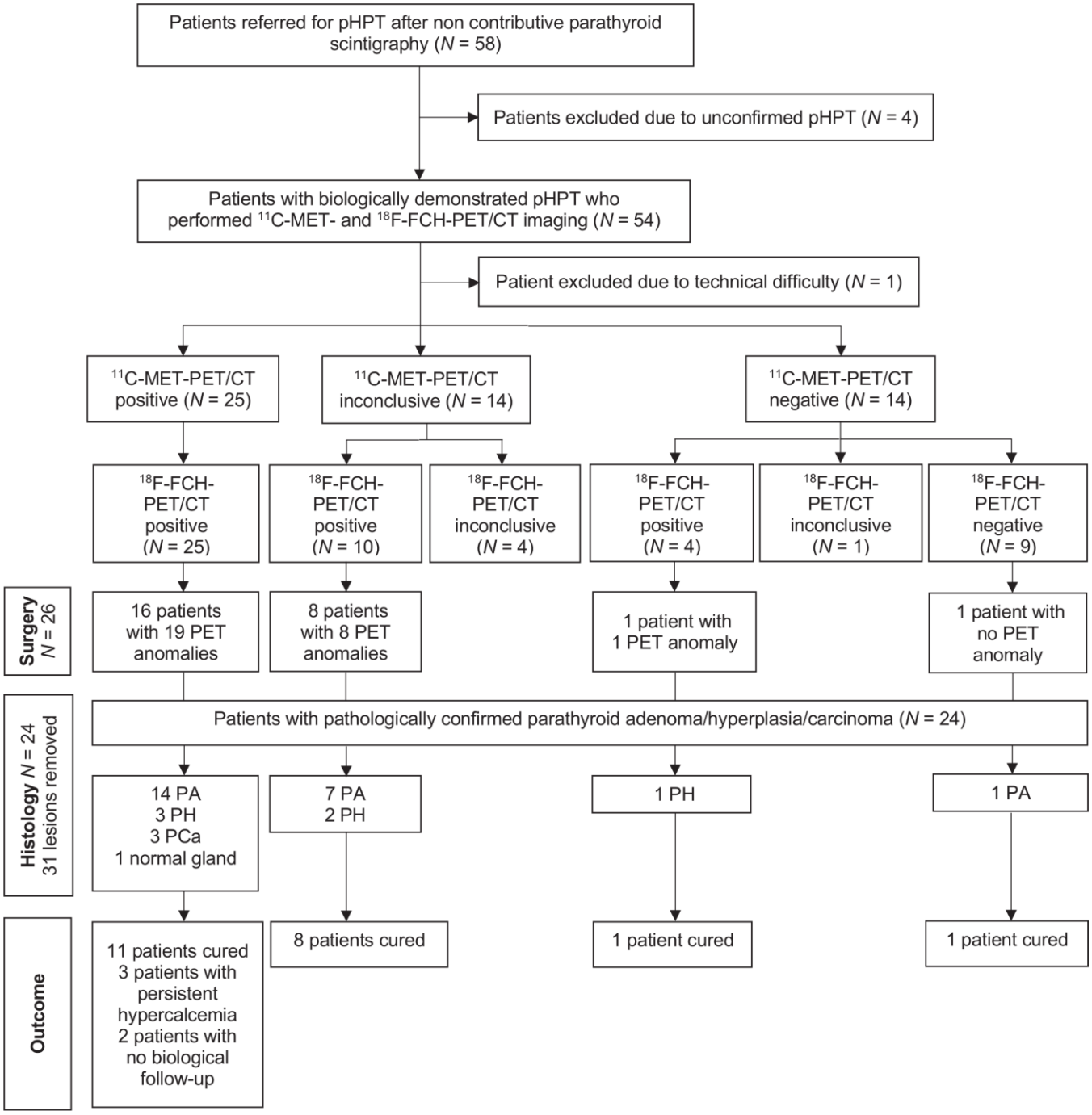

FIGURE 1 – Flow chart

^{18}F-FCH=^{18}F-Fluorocholine, ^{11}C-MET=^{11}C-Methionine, PA=parathyroid adenoma, PCa=parathyroid carcinoma, PH=parathyroid hyperplasia, pHPT=primary hyperparathyroidism

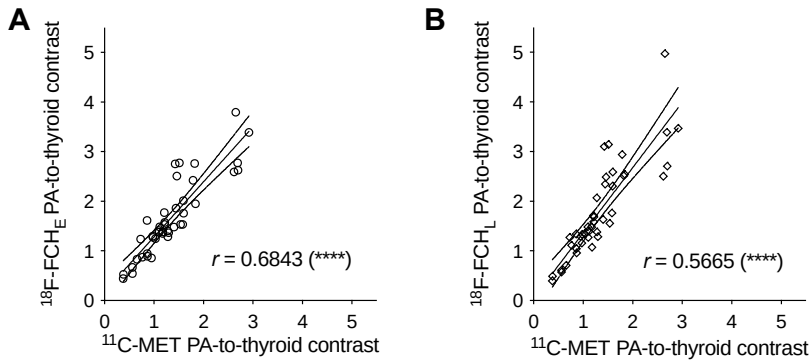

FIGURE 2 – Correlation between ^{18}F-FCH and ^{11}C-MET uptake

^{18}F-FCH($_{E/L}$)= ^{18}F-Fluorocholine (early/late), ^{11}C-MET=^{11}C-Methionine, PA=parathyroid adenoma

****, p<0.0001

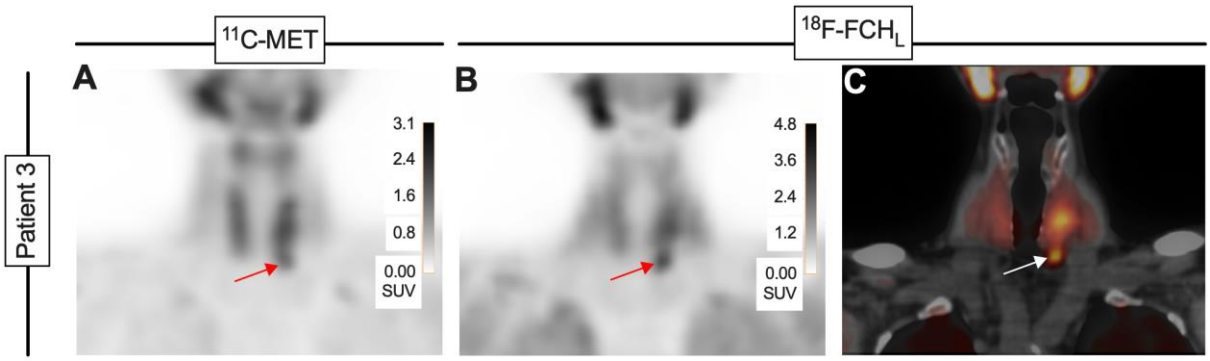

FIGURE 3 – Patient 3

Coronal PET/CT images of a 67 y-old female patient with pHPT and an inconclusive MIBI SPECT/CT (doubtful right inferior focus). (A) ^{11}C-MET images show asymmetrical thyroid lobes with a lower extension on the left (red arrow). (B) ^{18}F-FCH$_L$ images shows nodular uptake under the base of the left thyroid lobe (red arrow). (C) PET/CT fused images detailed the nodular aspect of the ^{18}F-FCH uptake (white arrow) in a parathyroid adenoma confirmed at histopathological analysis.

^{18}F-FCH$_L$=^{18}F-Fluorocholine late, ^{11}C-MET=^{11}C-Methionine, MIBI=^{99m}Tc-sestaMIBI SPECT scintigraphy, PTH=parathyroid hormone, pHPT=primary hyperparathyroidism

GRAPHICAL ABSTRACT

^{18}F-fluorocholine PET/CT compared to **^{11}C-methionine** PET/CT for the localization of hyperfunctioning **parathyroid** tissue

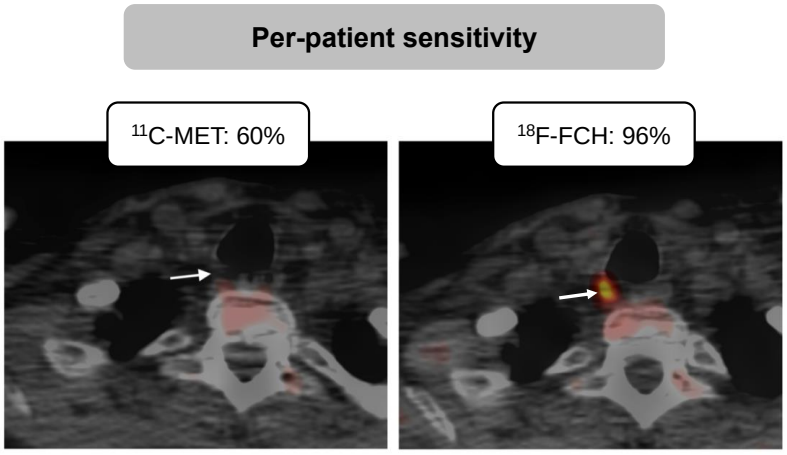

SUPPLEMENTARY MATERIALS

Supplemental TABLE 1

PET/CT results in function of biology, history, localization and histopathology

	Ca	P	PTH	History	Previous imaging	^{11}C-MET	^{18}F-FCH$_E$	^{18}F-FCH$_L$	Surgical localization	Histology
P1	2.76	0.68	95			2	2	2	P4R	PA
P2	2.66	0.92	53			0	2	2		
P3	2.79	0.9	140		US	0	0	0		
P4	2.58	0.87	71	GH macroadenoma	US	2/1/0/1	2/2/1/1	2/2/1/1	P3L	PH
P5	2.85	0.73	42	fracture	US/Neck CT	2	2	2	P4L	PA
P6	2.64	0.52	72	RC/hypercalciuria	US/Chest CT	2/1	2/2	2/2		
P7	2.81	0.87	49		US/Neck MRI	1	2	2	P3R	PA
P8†	3.0	NA	163	surgery	US	2	2	2	P3L	PA
P9*	2.57	0.87	48	surgery/RC	US	0	2	2	P3R	PH
P10	2.6	1.1	92	OP/hypercalciuria	US	0/0	2/1	2/1		
P11	2.72	0.56	71		US	1	1	1		
P12	2.57	0.55	61	CM/Crohn	US	0	2	2		
P13	2.94	0.36	150	RC/OP/hypercalciuria	US	2	2	2	P4R	PA
P14	2.75	0.78	29			0	0	0		
P15	2.64	0.53	46	surgery	US	0	0	0	P3R	PA
P17	2.97	0.75	160	hypercalciuria		2	2	0	Intrathyroidal R	PA
P20	2.62	0.71	50	hypercalciuria/Basedow	US	2	2	2	P3L	PA
P21*	2.88	0.86	81	RC/OP/hypercalciuria	US	2	2	2	P3L (+P4)	PA (+ 2 PH)
P22	3.23	0.63	530			2	2	2	P3R	PA
P23	2.6	0.88	73	OP/hypercalciuria	US/Neck CT	1	2	2		
P24	2.56	0.99	43	Thyroid surgery		0	1	1		
P25	2.88	0.99	142		US	1	2	2	ectopic	PA (+ PH)
P26	2.67	0.63	52	RC/OP/Hashimoto	US	1	2	2	P3L	PH
P27	2.85	0.95	40		US	1	2	2	P3R	PA
P28	2.64	0.85	88	RC/hypercalciuria	US	1	2	2	P3R	PA
P29	2.7	0.87	72	Hashimoto	US/Neck CT	1	1	2	P3L	PA
P30	2.82	0.74	54	hypercalciuria		2/2/0	2/2/0	2/2/1		

P32	2.77	0.45	54	OP		2	2	2	P4L	PA
P33	2.74	0.73	70		US	2	2	2	P3L	PA
P34	2.65	0.70	60	CM	US/Neck CT	0	0	0		
P35	2.51	0.77	56	hypercalciuria	US/Neck CT	0	0	0		
P36	2.59	0.73	150	OP		2	2	2		
P37	3.35	0.66	62	OP/pancreatitis	*NA*	1	2	2	ectopic	PA
P38	2.87	0.44	100		US	2	2	2	P3R	PCa
P39	2.54	0.72	64	OP	US	2	2	2		
P40	2.47	0.69	73	OP/hypercalciuria	US/Neck CT	0	1	1		
P41	2.51	0.94	78	CM/hypercalciuria	US	0	0	0		
P42	2.82	0.96	77			0	0	0		
P43	2.66	0.99	244		*NA*	2/1	2/2	2/2		
P44	2.50	0.92	40	CM	US	1	2	2	P3R	PA
P45	2.67	0.69	62	HIV	US	0	0	0		
P46	2.67	0.67	96	surgery	*NA*	2	2	2		
P47	2.76	0.64	106	OP/hypercalciuria/crohn	US	0	0	0		
P49	2.67	0.67	79	Surgery/OP/pheochromocytoma		2	2	2	P4R	PA
P50*	2.63	0.59	114		Chest CT	2/0/0	2/2/2	2/2/2	P3R/ P4R/ P4L	3 PA
P51	2.71	0.82	101	surgery	US	2	2	2	P3R	Normal gland
P52	2.59	0.7	116	hypercalciuria		2	2	2		
P53	2.65	1.05	49	surgery		2	2	2		
P54	2.65	0.35	279	CM/breast-ovarian cancer	US	2/2/2	2/2/2	2/2/2	P3L/ Intrathyroidal L	bifocal PCa/ unexplored R
P55	2.77	0.70	55	hypercalciuria	*NA*	0	1	1		
P56	2.65	0.84	133		US	1	2	2		
P57	2.78	0.77	51		US	2	2	2		
P58	2.62	0.69	35	RC/OP	US	1	1	0		

Px=patient x, Ca=serum calcium, P=serum phosphorus, PTH=parathyroid hormone, GH= growth hormone, RC=renal colic, CM=calcimimetic drug, surgery=parathyroidectomy, OP=osteopenia/-porosis, US=neck ultrasonography, CT= CT scanner, MRI=magnetic resonance imaging, NA=not available, ^{11}C-MET=^{11}C-Methionine, ^{18}F-FCH$_{E/L}$=^{18}F-Fluorocholine early/late, Scores 0=negative; 1=inconclusive; 2=positive, P3=inferior parathyroid gland, P4=superior parathyroid gland, R=right, L=left, PA=parathyroid adenoma, PH=parathyroid hyperplasia, PCa=parathyroid carcinoma

***** Patients with familial context of multiple endocrine neoplasia or other rare syndrome

Supplemental TABLE 2

Contingency Tables for ^{18}F-FCH vs. Histology and ^{11}C-MET vs. Histology

Per lesion resected	**Positive ^{18}F-FCH**	**Negative ^{18}F-FCH**	**Total ^{18}F-FCH**
PA	21	1	22
PH	3*	3	6
PCa	3	0	3
Total	27	4	31

* mismatch in location for a lesion

Sensitivity = 26 / 31 = 84%

PPV = 26 / 29 (FP: 1mismatch localization, 1 normal gland, 1 thyroid nodule) = 89.6%

Specificity, NPV, Accuracy: NA

Per lesion resected	**Positive ^{11}C-MET**	**Negative ^{11}C-MET**	**Total ^{11}C-MET**
PA	12	10	22
PH	1	5	6
PCa	3	0	3
Total	16	15	31

Sensitivity = 16 / 16 + 15 = 52%

PPV = 16 / 16 + 1 (normal gland) = 94%

Specificity, NPV, Accuracy: NA

PA=parathyroid adenoma, PH=parathyroid hyperplasia, PCa=parathyroid carcinoma, ^{18}F-FCH=^{18}F-Fluorocholine, ^{11}C-MET=^{11}C-Methionine, NA=non applicable

Supplemental TABLE 3

Pitfalls in PET/CT	^{11}C-MET	^{18}F-FCH
Lymph nodes	+	+
Mediastinal tumor	+	+
Thyroid nodule		+
Oesophagus	+	

^{11}C-MET=^{11}C-Methionine; ^{18}F-FCH=^{18}F-Fluorocholine

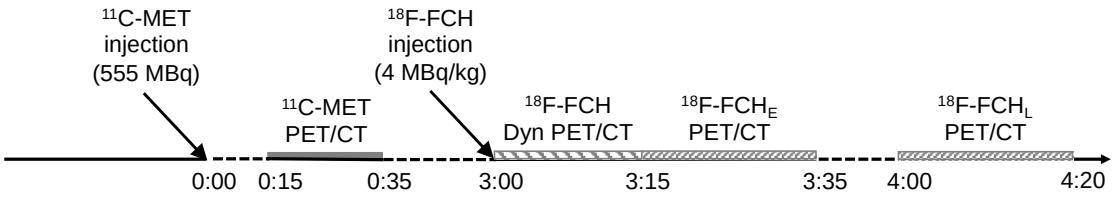

Supplemental FIGURE 1 – One-day imaging timeline

Dyn=dynamic, ^{18}F-FCH($_{E/L}$)= ^{18}F-Fluorocholine(early/late), MBq=Megabecquerel, ^{11}C-MET=^{11}C-Methionine

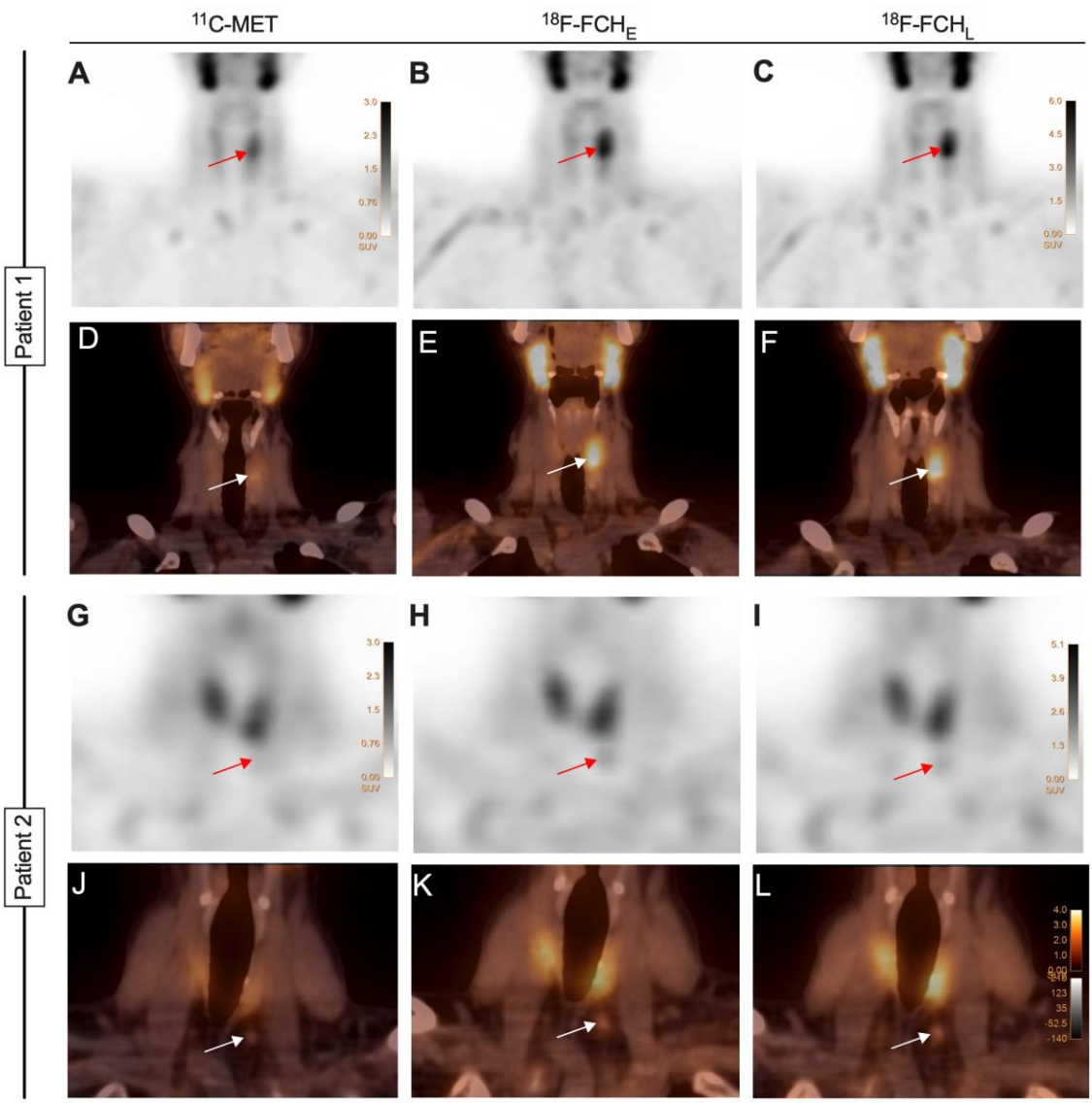

Supplemental FIGURE 2 –

Patient 1: Coronal PET images (A-D) ^{11}C-MET (B-E) ^{18}F-FCH$_E$ and (C-F) ^{18}F-FCH$_L$ in a 52 y-old female patient with pHPT and negative MIBI SPECT/CT. Moderate ^{11}C-MET uptake and intense ^{18}F-FCH uptake (arrows) of a voluminous nodule behind the upper left pole, with a slightly better contrast on late ^{18}F-FCH images.

Patient 2: (G) ^{11}C-MET compared to (H-I) ^{18}F-FCH$_E$ and ^{18}F-FCH$_L$ and respective (J-K-L) fusion images for detection of parathyroid lesion of a 68 y-old female patient with pHPT with negative MIBI SPECT/CT. Negative ^{11}C-MET-PET/CT but positive early and late ^{18}F-FCH-PET/CT.

^{18}F-FCH$_{(E/L)}$= ^{18}F-Fluorocholine (early/late), ^{11}C-MET=^{11}C-Methionine, MIBI=^{99m}Tc-sestaMIBI SPECT scintigraphy, pHPT=hyperparathyroidism

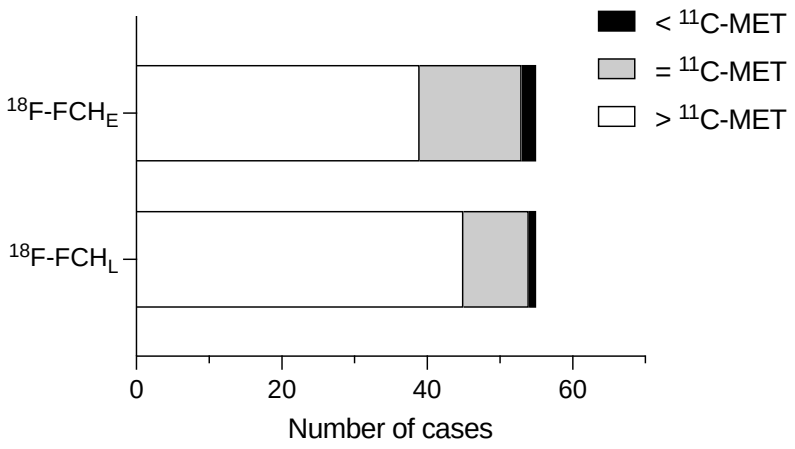

Supplemental FIGURE 3 – Visual comparison to ^{11}C-MET uptake on ^{18}F-FCH$_E$ vs. ^{18}F-FCH$_L$

^{18}F-FCH$_{(E/L)}$= ^{18}F-Fluorocholine (early/late), ^{11}C-MET=^{11}C-Methionine

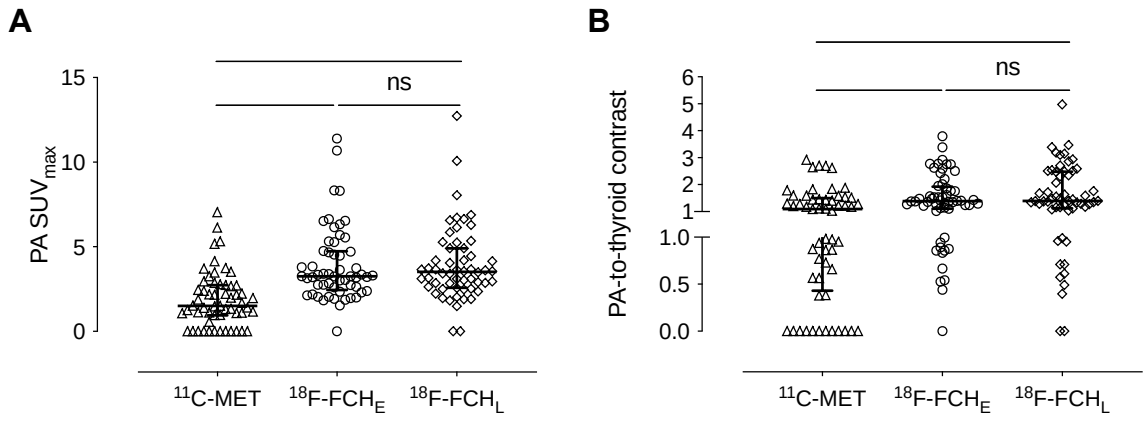

Supplemental FIGURE 4 – Distribution of SUVmax PA and PA/Thyroid

^{18}F-FCH$_{(E/L)}$= ^{18}F-Fluorocholine(early/late), ^{11}C-MET=^{11}C-Methionine, PA=parathyroid lesion
****, p<0.0001